Optical simulation of Markovian quantum channels

Marcello H. Passos[1,2], Paola C. Obando[1], Fagner M. Paula[3], José A.O. Huguenin[1,2]

[1]Instituto de Física, Universidade Federal Fluminense (UFF)
Av. Gal. Milton Tavares de Souza s/n, Gragoatá, 24210-346, Niterói, RJ – Brasil

[2]Instituto de Ciências Exatas, Universidade Federal Fluminense (UFF)
Rua De. Ellis Hermydio Figureia, 783, 27213-145, Volta Redonda - RJ - Brasil

[3]Centro de Ciências Naturais e Humanas, Universidade Federal do ABC (UFABC)
Avenida dos Estados 5001, 09210-580, Santo André, São Paulo – Brasil

{marcellopassos123,paolaconcha05, fagnermuruci}@gmail.com, jose_huguenin@id.uff.br

Abstract. *We present an implementation an experimental simulation of quantum channels by using an all-optical setup where the qubit was encoded in polarization degree of freedom and the environment was encoded in the propagation path degree of freedom. The experiment is a test bed for theoretical investigation of quantum decoherence processesing Markovian quantum channels.*

Resumo. *Neste trabalho, apresentamos a realização da simulação experimental de canais quânticos usando circuitos ópticos onde o qubit foi codificado no grau de liberdade de polarização e o ambiente foi codificado no grau de liberdade do caminho. Esse experimento é uma plataforma para realização de testes na investigação teórica do processo de decoerência quântica no em canais quânticos Markovianos.*

1. Introduction

Quantum communication and Quantum Computation present a hard challenge: decoherence process due inevitable interaction of qubits with the environment in quantum channels [Nielsen and Chuang 2001]. Indeed, Coherence is a very important resource for the quantum information theory and contributes to the advancement of quantum information processing [Bagan et al. 2016].

Developed originally in quantum optics domain [Glauber 1963], nowadays, the theory of quantum coherence presents a intense research field that consists to quantifying coherence for general states once coherence is regarded as an operational resource [Baumgratz et al. 2014].

Concerning the decoherence, an important phenomena observed is the freezing of coherence, that's consist in time invariance of the quantum system that evolves under noisy dynamics without external control [Bromley et al. 2015]. We recover this effect in our optical simulation.

Simulation of quantum systems by means linear optical circuits are an intense research field. We can cite studies of topological phases in the evolution of a pair of entangled qubits [Souza et al. 2007], Bell's inequality [Borges et al. 2010], Mermin's inequality for entangled tripartite system [Balthazar et al. 2016], cryptography

[Souza et al. 2008], teleportation [da Silva et al. 2016], and simulation of quantum gates [Balthazar and Huguenin 2016].

In Ref. [Obando et al. 2020] we present a complete theoretical and experimental studies on quantum decoherence processes, by considering a single qubit in Markovian channels. In the present work we focus on the presentation of the experimental simulation of Amplitude Damping (AD) and Bit Flip (BF) channels.

2. Optical simulation of quantum channels

The system and reservoir are encoded in degree of freedom of light, more specifically an intense laser beam. The qubit representing the system are encoded in polarization degree of freedom in such way we have $|H\rangle \equiv |0\rangle_S$(system ground state) and $|V\rangle \equiv |1\rangle_S$(system excited state). The reservoir is encoded in the propagation path (orthogonal directions), labeled as $|0\rangle_R$ and $|1\rangle_R$.

Figure 1 presents the experimental setup. A DPSS laser (horizontally polarized) $(532nm, 1.5mw$ power) passes through a half wave plate with its fast axis making an angle of θ_1 with the horizontal (HWP1@θ_1). The initial polarization state can be written as

$$|\psi_i\rangle = |\psi(\theta_1)\rangle_S = cos(2\theta_1)|H\rangle_s + sin(2\theta_1)|V\rangle_S. \quad (1)$$

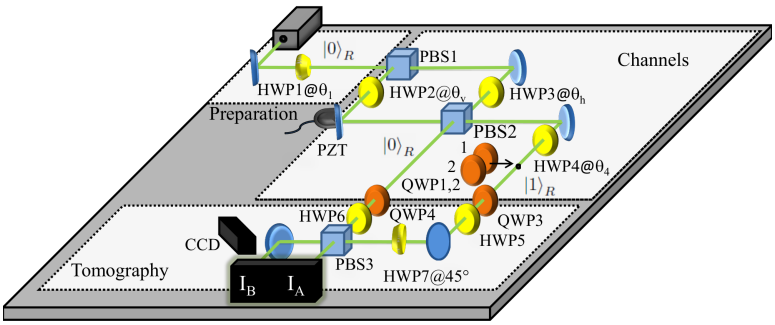

Figure 1. Experimental setup. HWP for half wave plate, QWP for quarter wave plate, PBS for polarizing beam splitter, PZT for piezoelectric ceramic, and CCD for Charge-Coupled Device camera.

Setting θ_1, we can write different initial states. For instance, If $\theta_1 = \pi/8$, we have a $+45°$ polarized beam that is the analog of the maximally coherent state $|\psi(\pi/8)\rangle_S \equiv |+\rangle_S = \frac{1}{\sqrt{2}}(\,|H\rangle + |V\rangle\,)$ [Passos et al. 2018]. For $\theta_1 = \pi/4$ we have a vertically polarized beam stated as $|\psi_V\rangle_S \equiv |1\rangle_S = |V\rangle$. For system-reservoir state, the initial propagation path is associated to the reservoir ground state. Then we can write that after HWP1 we have initial state the state $|\psi_\beta\rangle_S|0\rangle_R$ where $\beta = +, V$.

The quantum channels are simulated by the optical circuit presented in the block "Channels" and follows Ref. [Salles et al. 2008]. For any initial state shining PBS1, H-polarization component is transmitted and the V-polarization reflected. For V-component, half wave plate HWP2@θ_v has its fast axis performing an angle θ_v with the vertical direction. For H-component, another half wave plate HWP3@θ_h has its fast axis performing an angle θ_h with the horizontal. The two arms are recombined in PBS2. For $\theta_v = \theta_h = 0$ the

polarization components H and V leaves PBS2 in the same port (the path associated with the reservoir ground state $|0\rangle_R$). For θ_v or/and θ_h different from zero, the path associated with the reservoir excited state $|1\rangle_R$ present non zero intensity.

In this path we have an additional half wave plate HWP4@θ_4. A phase difference $\phi = \phi_2 - \phi_1$ between the paths $|0\rangle_R$ and $|1\rangle_R$ can be controled by using a couple of quarter waves plates QWP1@ϕ_1 and QWP2@ϕ_2 that are inserted or removed in the path $|1\rangle_R$. In association with combinations of θ_v, θ_h, and θ_4, we can emulates different quantum channels [Salles et al. 2008].

As we need density matrix ρ polarization states after the channels in order to calculate coherence, tomographic measurements is preformed in the last part of the circuit ("Tomography" block).

The Quantum Coherence ($C(\rho)$) and the Maximum Coherence ($C_{max}(\rho)$) are given by [Obando et al. 2020]

$$C(\rho) = \sum_{s,s'(s\neq s')} |\langle s|\rho|s'\rangle|, \tag{2}$$

$$C_{max}(\rho) = \sum_{s,s'} |\langle s|\rho - I/d|s'\rangle|, \tag{3}$$

with I denoting the identity operator. For one-qubit ($d = 2$) in the computational basis, the density operator presents the form $\rho = (I + \vec{r}.\vec{\sigma})/2$, where $\vec{r} = (r_x, r_y, r_z)$. Then we can compare our experimental results with quantum theory.

It is worth to mention that $C_{max}(\rho)$ is related with the purity of the state while $C(\rho)$ is ssociated to the level of superposition, for instance, the state $|+\rangle = \frac{1}{\sqrt{2}}(|0\rangle + |1\rangle)$ presents $C(\rho) = C_{max}(\rho) = 1$. However, for the state $|V\rangle$, $C(\rho) = 0$, there is no superposition and $C_{max}(\rho) = 1$, we have a pure state.

3. Experimental results

In this section we present the results for the simulated channels. We present the simulation of Amplitude Damping and Bit Flip channels.

3.1. Amplitude Damping (AD) channel

We can emulate AD channel by setting $\theta_h = 0^\circ$, $\theta_v = \theta$, $\theta_4 = 0^\circ$ and we do not insert the QW plates. The transformation map can be written as

$$\begin{aligned} |\psi(\theta_1)\rangle_S\,|0\rangle_R \;&\rightarrow\; \cos(2\theta_1)\,|H\rangle_S|0\rangle_R \,+\sin(2\theta_1)[\cos(2\theta)|V\rangle_S|0\rangle_R \\ &+\; \sin(2\theta)\,|H\rangle_S\,|1\rangle_R]. \end{aligned} \tag{4}$$

.

By comparing with the map of the AD channel, we can recognize the relation of θ and the time dependent probability $p(t)$ as [Obando et al. 2020]

$$cos(2\theta) = \sqrt{1 - p(t)}, \tag{5}$$

in such way we can relate t with θ and reproduce the qubit dynamics along the channel.

For an initial state $|\psi(\theta_1)\rangle_S = |V\rangle_S$, that is, $\theta_1 = \pi/4$, we have

$$|\psi(\pi/4)\rangle_S = [cos(2\theta)|V\rangle_s \otimes |0\rangle_R + sin(2\theta)|H\rangle_S \otimes |1\rangle_R] \,. \tag{6}$$

For $\theta = 0$, that corresponding $t = 0$, the system and reservoir are in the intial state. For $\theta = \pi/4$, that corresponding $t \to \infty$, the sytem decay and the reservoir gains a quantum of energy. In our approach, the laser beam transform its polarization from V to H.

For an initial state $|\psi(\theta_1)\rangle_S = |+\rangle_S$, that is, $\theta_1 = \pi/8$, we have

$$\begin{aligned} |\psi(\pi/8)\rangle_S &= \frac{1}{\sqrt{2}} cos(2\theta)|H\rangle_s \otimes |0\rangle_R \\ &+ \frac{1}{\sqrt{2}} \left[\cos(2\theta)|V\rangle_S|0\rangle_R + \sin(2\theta)\ |H\rangle_S\ |1\rangle_R\right] . \end{aligned} \tag{7}$$

By re-writing regrouping reservoir states, we have

$$\begin{aligned} |\psi(\pi/8)\rangle_S &= cos(2\theta)\frac{[|H\rangle_s + |V\rangle_s]}{\sqrt{2}} \otimes |0\rangle_R \\ &+ \frac{1}{\sqrt{2}} \sin(2\theta)\ |H\rangle_S\ |1\rangle_R. \end{aligned} \tag{8}$$

For $\theta = 0$ ($t = 0$) the system and reservoir are in the initial state $|+\rangle_s \otimes |0\rangle_R$. For $\theta = \pi/4$, ($t \to \infty$), the system decay and the reservoir gains a quantum of energy. In our approach, the laser beam transform its polarization from $+45^\circ$ to H.

Figure 2 show the result for variation of θ for both illustrated initial states. Squares and triangles dots are experimental points while solid and dashed line are the respective theoretical quantum previsions. Fig. 2(a) presents $C(t)$ and $C_{max}(t)$ for the initial state $|\psi_i\rangle = |V\rangle$. As we can see, $C(t)$ is null for all t once no coherent superposition is present. For C_{max} we observe a frozen in the maximum value after passing by a minimum ($C_{max} = 0$ see inset in Fig. 2(a)). Note that before decaying to $|H\rangle$, the system state became a mixed state.

For the initial state $|\psi_i\rangle = |+\rangle$ (Fig. 2(b)), we have a lose of the coherent superposition and $C(t)$ decay fast to zero, as expected. On the other hand, C_{max} (Fig.2(b)) presents a minimum ($C_{max} = 0.87$) before frozen again. Our experimental results are in excellent agreement with quantum theory.

3.2. Bit Flip (BF) channel

Bit Flip (BF) channel is simulated by setting $\theta_h = -\theta,\ \theta_v = \theta,\ \theta_4 = 0^\circ$ and, again, we do not insert the QW plates. The results for BF channel is presented in Fig.3 for the initial state $|V\rangle$ (a) and $|+\rangle$ (b). Here we present the graphic as function of p, not γt.

For the initial state $|\psi_i\rangle = |V\rangle$, (Fig. 3(a)), we can see that that quantum coherence $C(p)$ remains equal to zero as expected. For $p = 0$ we have $C_{max}(0) = 1$ once we have a pure state. For $p = 0.5$ we have the mixed state for BF channel, leading to $C_{max} = 0$. For $p = 1$, the BF channel has as final state $|H\rangle$ that are a pure states and we recover $C_{max} = 1$.

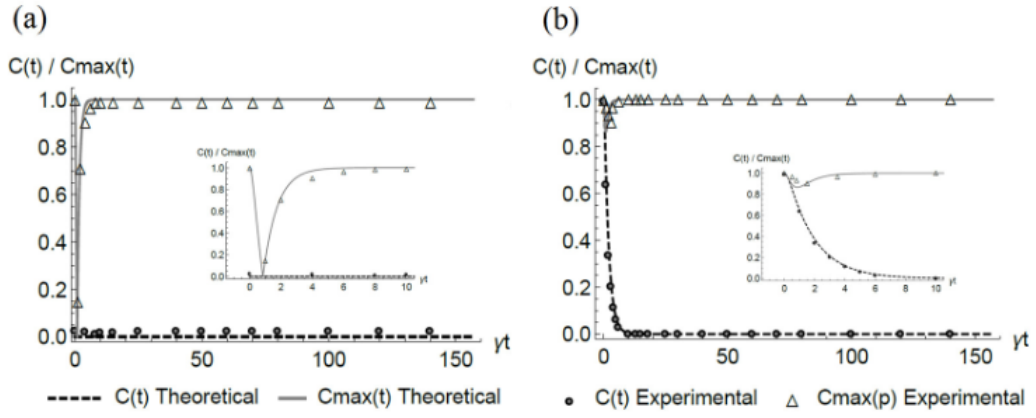

Figure 2. Quantum coherence (C) and maximal coherence (C_{max}) evolution in the AD channel for the initial state $|V\rangle$ (a) and $|+\rangle$.

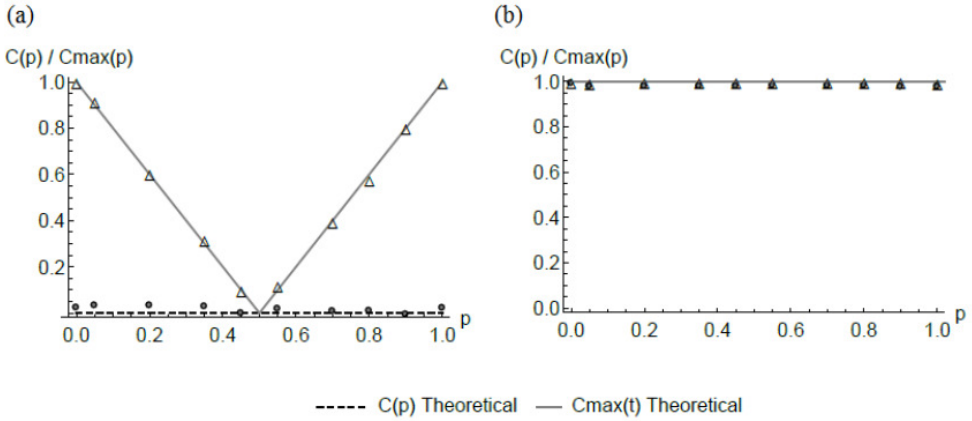

Figure 3. Quantum coherence (C) and maximal coherence (C_{max}) evolution in the BF channel for the initial state $|V\rangle$ (a) and $|+\rangle$ (b).

Now, for the initial state $|\psi_i\rangle = |+\rangle$, Fig. 3(b))shows the variation of $C(p)$ and $C_{max}(p)$. Such as state is pure and presents maximal superposition. Then, for $p = 0$ both coherence $C(0)$ and $C_{max}(0)$ are maximal. We can observe that for BF channel both coherence $C(p)$ and $C_{max}(p)$ were frozen and we do not have loss of superposition and purity, as expected [Obando et al. 2020].

All experimental results are in entire agreement with the quantum mechanics predictions.

4. Concluding remarks

We presented an experimental simulation of quantum channels exploring polarization degree of freedom of an intense laser beam by means a linear optical circuit. We performed the simulation of the Amplitude Damping (AD) and bit flip (BF) channels. It was possible to observe frozen behavior of Quantum Coherence and Maximal Coherence. All results are in excellent agreement with quantum mechanics prediction. This work is an experimental view of a complete study (theoretical and experimental) presented

in Ref.[Obando et al. 2020]. Here, we reinforce that linear optical circuits associated to intense laser beams is an excellent bed test for the evolution of quantum properties in quantum channels.

References

Bagan, E., Bergou, J. A., Cottrell, S. S., and Hillery, M. (2016). Relations between coherence and path information. *Physical review letters*, 116(16):160406.

Balthazar, W. and Huguenin, J. (2016). Conditional operation using three degrees of freedom of a laser beam for application in quantum information. *JOSA B*, 33(8):1649–1654.

Balthazar, W., Souza, C., Caetano, D., Galvão, E., Huguenin, J., and Khoury, A. (2016). Tripartite nonseparability in classical optics. *Optics letters*, 41(24):5797–5800.

Baumgratz, T., Cramer, M., and Plenio, M. B. (2014). Quantifying coherence. *Physical review letters*, 113(14):140401.

Borges, C., Hor-Meyll, M., Huguenin, J., and Khoury, A. (2010). Bell-like inequality for the spin-orbit separability of a laser beam. *Physical Review A*, 82(3):033833.

Bromley, T. R., Cianciaruso, M., and Adesso, G. (2015). Frozen quantum coherence. *Physical review letters*, 114(21):210401.

da Silva, B. P., Leal, M. A., Souza, C., Galvão, E., and Khoury, A. (2016). Spin–orbit laser mode transfer via a classical analogue of quantum teleportation. *Journal of Physics B: Atomic, Molecular and Optical Physics*, 49(5):055501.

Glauber, R. J. (1963). Coherent and incoherent states of the radiation field. *Physical Review*, 131(6):2766.

Nielsen, M. A. and Chuang, I. L. (2001). *Quantum computation and quantum information*, volume 2. Cambridge university press Cambridge.

Obando, P., Passos, M., Paula, F., and Huguenin, J. A. O. (2020). Simulating markovian quantum decoherence processes through an all-optical setup. *Quantum Information Processing*, 19(1):7.

Passos, M. H. M., Balthazar, W. F., Khoury, A. Z., Hor-Meyll, M., Davidovich, L., and Huguenin, J. A. O. (2018). Experimental investigation of environment-induced entanglement using an all-optical setup. *Physical Review A*, 97(2):022321.

Salles, A., de Melo, F., Almeida, M., Hor-Meyll, M., Walborn, S., Ribeiro, P. S., and Davidovich, L. (2008). Experimental investigation of the dynamics of entanglement: Sudden death, complementarity, and continuous monitoring of the environment. *Physical Review A*, 78(2):022322.

Souza, C., Borges, C., Khoury, A., Huguenin, J., Aolita, L., and Walborn, S. (2008). Quantum key distribution without a shared reference frame. *Physical Review A*, 77(3):032345.

Souza, C., Huguenin, J., Milman, P., and Khoury, A. (2007). Topological phase for spin-orbit transformations on a laser beam. *Physical review letters*, 99(16):160401.